Crossover between distinct mechanisms of microwave photoresistance in bilayer systems

S. Wiedmann,[1,2] G. M. Gusev,[3] O. E. Raichev,[4] A. K. Bakarov,[5] and J. C. Portal[1,2,6]
[1]*LNCMI-CNRS, UPR 3228, BP 166, 38042 Grenoble Cedex 9, France*
[2]*INSA Toulouse, 31077 Toulouse Cedex 4, France*
[3]*Instituto de Física da Universidade de São Paulo, CP 66318 CEP 05315-970, São Paulo, SP, Brazil*
[4]*Institute of Semiconductor Physics, NAS of Ukraine, Prospekt Nauki 41, 03028, Kiev, Ukraine*
[5]*Institute of Semiconductor Physics, Novosibirsk 630090, Russia*
[6]*Institut Universitaire de France, 75005 Paris, France*
(Received 10 November 2009; published 8 February 2010)

We report on temperature-dependent magnetoresistance measurements in balanced double quantum wells exposed to microwave irradiation for various frequencies. We have found that the resistance oscillations are described by the microwave-induced modification of electron distribution function limited by inelastic scattering (inelastic mechanism), up to a temperature of $T^* \simeq 4$ K. With increasing temperature, a strong deviation of the oscillation amplitudes from the behavior predicted by this mechanism is observed, presumably indicating a crossover to another mechanism of microwave photoresistance, with similar frequency dependence. Our analysis shows that this deviation cannot be fully understood in terms of contribution from the mechanisms discussed in theory.

DOI: 10.1103/PhysRevB.81.085311 PACS number(s): 73.40.−c, 73.43.−f, 73.21.−b

I. INTRODUCTION

The physics of two-dimensional (2D) electron systems exposed to a continuous microwave irradiation in the presence of perpendicular magnetic fields B has attracted both experimental and theoretical attention in the last years following the observation of the microwave-induced resistance oscillations (MIROs) (Ref. 1), which evolve into "zero resistance states" (ZRS) (Refs. 2 and 3) for a sufficiently high microwave intensity. The MIRO periodicity is governed by the ratio of the radiation frequency ω to the cyclotron frequency $\omega_c = eB/m$, where m is the effective mass of the electrons. These oscillations occur because of Landau quantization and originate from the scattering-assisted electron transitions between different Landau levels, which become possible in the presence of microwave excitation. Two competing microscopic mechanisms of the oscillating photoresistance have been proposed theoretically: the "displacement" mechanism which accounts for spatial displacement of electrons along the applied dc field under scattering-assisted microwave absorption,[4,5] and "inelastic" mechanism, owing to an oscillatory contribution to the isotropic part of the electron distribution function.[6,7] Both mechanisms describe phase and periodicity of MIROs observed in experiments. A systematic theoretical study of photoresistance has revealed two additional mechanisms: the "quadrupole" mechanism, which comes from excitation of the second angular harmonic of the distribution function, and "photovoltaic" mechanism, which is described as a combined action of the microwave and dc fields on both temporal and angular harmonics of the distribution function.[7] Both additional mechanisms contribute to transverse (Hall) dc resistance, while the photovoltaic mechanism contributes also to diagonal resistance. However, this contribution is found to be weak and has not been detected in MIROs observed in experiments.

For low temperatures, the inelastic mechanism plays the dominant role because the relaxation of the microwave-induced oscillatory part of the electron distribution is slow. This relaxation is governed by the inelastic electron-electron scattering with a characteristic time $\tau_{in} \propto T^{-2}$, which is in the order of 1 ns at temperatures $T \simeq 1$ K. This T^{-2}-dependence has also been found experimentally in Ref. 8. Nevertheless, recent experiments on high-mobility samples suggest that the displacement mechanism cannot be ignored and becomes important with increasing temperature, when the relative contribution of the inelastic mechanism decreases.[9] The crossover between these two mechanisms was observed at $T \simeq 2$ K. Notice that, since these mechanisms produce nearly the same frequency dependence of MIROs, the only way to distinguish between them is to measure temperature dependence of the oscillation amplitudes. For a better understanding of the role of inelastic and displacement mechanisms in microwave-induced resistance of 2D electrons, systematic experiments in different samples are highly desirable.

In this paper, we undertake a study of temperature dependence of magnetoresistance in two-subband electron systems formed in double quantum wells (DQWs). Recently, we have found[10] that the inelastic mechanism satisfactorily explains low-temperature photoresistance in such systems exposed to microwave irradiation. The main difference in magnetoresistance of two-subband electron systems with respect to conventional (single-subband) 2D systems is the presence of magneto-intersubband (MIS) oscillations (see Refs. 11–13 and references therein) which occur owing to periodic modulation of the probability of intersubband transitions by the magnetic field. Under microwave irradiation, these oscillations interfere with MIROs. The interference causes a peculiar magnetoresistance picture where one may see enhancement, suppression, or inversion (flip) of MIS peaks, correlated with the microwave frequency.[10] Whereas such a behavior of magnetoresistance is more complicated than that for single-subband electron systems, it offers certain advantages in analyzing the effect of microwaves. The reason is that the quantum component of magnetoresistance, which is affected by the microwaves, is "visualized" in DQWs by the MIS oscillations whose period is typically smaller than the period of the MIROs. As a result, the changes in MIRO amplitudes caused by variation in temperature or microwave

intensity can be traced by observation of the behavior of single MIS peaks, and the position of node points of the MIROs can be determined more distinctly by the MIS peak inversion.

Our main result can be summarized as follows. We find that the inelastic mechanism fails to explain the observed photoresistance for $T>4$ K. The temperature dependence of magnetoresistance can be explained either by a deviation from the $\tau_{\rm in}\propto T^{-2}$ law at these temperatures or by inclusion of another, T-independent contribution to MIROs. The first possibility seems to be unlikely, because we see no reasons for such a deviation. The second possibility is more promising, and a consideration of an additional contribution owing to the displacement mechanism seems to be a natural choice. However, our quantitative estimates demonstrate that the crossover from the inelastic to the displacement mechanism of MIROs is expected at higher temperatures in our samples, around 10 K. Therefore, the origin of the observed photoresistance behavior can be partially explained by a contribution of displacement mechanism but does not fully account for our finding.

The paper is organized as follows. In Sec. II, we present details of the experimental analysis and the theoretical consideration of the microwave-induced resistivity of two-subband systems. In Sec. III, we analyze the deviation from the inelastic mechanism with increasing temperature, compare our experimental results with the theory including both inelastic and displacement mechanisms, and formulate our conclusions.

II. EXPERIMENTAL AND THEORETICAL BASIS

We have studied balanced GaAs DQWs separated by different $Al_xGa_{1-x}As$ barriers with barrier thicknesses of $d_b=14$, 20, and 30 Å in perpendicular magnetic fields. We have analyzed two wafers with $d_b=14$ Å and we focus in this paper on the samples with subband separation of $\Delta=3.05$ meV. This value is extracted from the periodicity of low-field MIS oscillations. The samples have a high total sheet electron density $n_s\simeq 1.15\times 10^{12}$ cm^{-2} and a mobility of $\mu\simeq 1.4\times 10^6$ cm^2/V s at 1.4 K. The measurements have been carried out in a VTI cryostat using conventional lock-in technique to measure the longitudinal resistance $R=R_{xx}$ under a continuous microwave irradiation. As MW sources, we employ different "carcinotron" generators and we focus on the frequency range between 55 and 140 GHz. A circular section waveguide delivers microwave radiation down to the sample, which is placed at a distance of 1–2 mm in front of the waveguide output.

In Fig. 1, we present the basis of our experimental analysis for further temperature-dependent measurements. Without microwaves (no mw), we observe MIS oscillations, which are superimposed on low-field Shubnikov-de Haas (SdH) oscillations at low temperatures. As the microwave power increases (at a fixed microwave frequency of 85 GHz), the MIS oscillation picture is modified by the MIRO contribution. It is worth mentioning that we have to perform the experimental analysis for low microwave intensity to ensure that the amplitude of MIS peaks is not yet saturated. Thus,

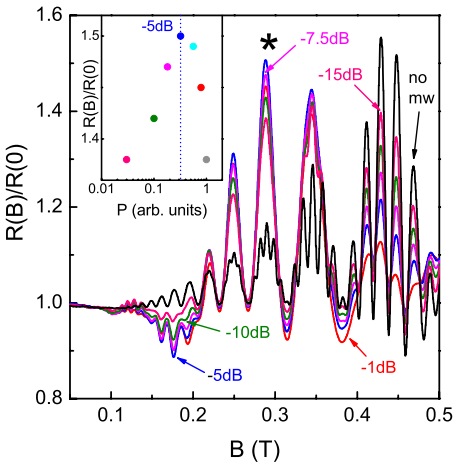

FIG. 1. (Color online) Normalized power dependent photoresistance as a function of the magnetic field for 85 GHz at $T=1.4$ K. Without microwave irradiation (no mw), MIS oscillations are visible, superimposed on SdH oscillations. An increase in microwave intensity leads to an enhancement, damping, or flip of MIS peaks. We observe a saturation of the MIS oscillation for the attenuations between −2.5 and −5 dB; the inset shows the amplitude of the MIS peak marked with an asterisk.

we present in Fig. 1 power dependent measurements for several chosen attenuations: 0, −1, −2.5, −5, −7.5, −10, and −15 dB. The inset to Fig. 1 shows MIS peak amplitude at $B=0.3$ T (marked by an asterisk) where saturation occurs between −2.5 and −5 dB. Therefore, we use experimental data with lower microwave intensity (for this frequency $P\leq -7.5$ dB). Still, the heating of 2D electrons by microwaves is observable at these intensities by a suppression of SdH oscillations. This heating is not strong and does not lead to the bolometric effect at $\omega_c\simeq\omega$ because of the radiative broadening of the cyclotron resonance.[8,14] For temperatures below 10 K, the phonon-induced contribution to electron mobility in our samples is weak, so the transport is controlled by the electron-impurity scattering.

Our theoretical model takes into account both inelastic and displacement mechanisms of photoresistance generalized to the two-subband case (for generalization to an arbitrary number of subbands, see Ref. 15). In the regime of classically strong magnetic fields, the symmetric part of the diagonal resistivity, ρ_d, in the presence of microwaves is given by the expression

$$\frac{\rho_d}{\rho_0}=1-2\mathcal{T}\tau_{\rm tr}\sum_{j=1,2}\nu_j^{\rm tr}d_j\cos\frac{2\pi(\varepsilon_F-\varepsilon_j)}{\hbar\omega_c}+\tau_{\rm tr}\left[\sum_{j=1,2}\frac{2n_j}{n_s}\nu_{jj}^{\rm tr}d_j^2+2\nu_{12}^{\rm tr}d_1d_2\cos\frac{2\pi\Delta}{\hbar\omega_c}\right]-\frac{1}{2}\tau_{\rm tr}^2A_\omega\left[\sum_{j=1,2}(\nu_j^{\rm tr}d_j)^2+2\nu_1^{\rm tr}\nu_2^{\rm tr}d_1d_2\cos\frac{2\pi\Delta}{\hbar\omega_c}\right]-\tau^*B_\omega\left[\sum_{j=1,2}\left(\frac{2n_j}{n_s}\right)^2\nu_{jj}^*d_j^2+2\nu_{12}^*d_1d_2\cos\frac{2\pi\Delta}{\hbar\omega_c}\right],\quad(1)$$

where the sums are taken over the subbands $j=1,2$ with energies ε_j separated by $\Delta=|\varepsilon_2-\varepsilon_1|$. The second term is the first-order quantum correction describing the SdH oscillations ($\varepsilon_F=\hbar^2\pi n_s/2m$ is the Fermi energy), and the third term is the equilibrium second-order quantum correction containing the MIS oscillations. The fourth and the fifth terms are nonequilibrium second-order quantum corrections describing the influence of microwaves owing to inelastic and displacement mechanisms, respectively. In Eq. (1), $\rho_0=m/e^2n_s\tau_{\rm tr}$, $\tau_{\rm tr}$ is the averaged transport time defined as $1/\tau_{\rm tr}=(\nu_1^{\rm tr}+\nu_2^{\rm tr})/2$, $1/\tau^*=(\nu_1^*+\nu_2^*)/2$, $d_j=\exp(-\pi\nu_j/\omega_c)$ are the Dingle factors, $\mathcal{T}=X/\sinh X$ with $X=2\pi^2T/\hbar\omega_c$ is the thermal suppression factor, and n_j are the partial densities in the subbands ($n_1+n_2=n_s$). The subband-dependent quantum relaxation rates ν_j and $\nu_{jj'}$, as well as the scattering rates $\nu_j^{\rm tr}$, ν_j^*, $\nu_{jj'}^{\rm tr}$, and $\nu_{jj'}^*$ are defined according to

$$\nu_j=\sum_{j'=1,2}\nu_{jj'},\quad \nu_j^{\rm tr}=\sum_{j'=1,2}\frac{n_j+n_{j'}}{n_s}\nu_{jj'}^{\rm tr},$$

$$\nu_j^*=\sum_{j'=1,2}\left(\frac{n_j+n_{j'}}{n_s}\right)^2\nu_{jj'}^*, \tag{2}$$

and

$$\left.\begin{matrix}\nu_{jj'}\\ \nu_{jj'}^{\rm tr}\\ \nu_{jj'}^*\end{matrix}\right\}=\int_0^{2\pi}\frac{d\theta}{2\pi}\nu_{jj'}(\theta)\times\left\{\begin{matrix}1\\ F_{jj'}(\theta)\\ F_{jj'}^2(\theta)\end{matrix}\right.,$$

$$\nu_{jj'}(\theta)=\frac{m}{\hbar^3}w_{jj'}(\sqrt{(k_j^2+k_{j'}^2)F_{jj'}(\theta)}), \tag{3}$$

where $w_{jj'}(q)$ are the Fourier transforms of the correlators of the scattering potential, $F_{jj'}(\theta)=1-2k_jk_{j'}\cos\theta/(k_j^2+k_{j'}^2)$, θ is the scattering angle, and $k_j=\sqrt{2\pi n_j}$ is the Fermi wavenumber for subband j. Next,

$$A_\omega\simeq\frac{\mathcal{P}_\omega(2\pi\omega/\omega_c)\sin(2\pi\omega/\omega_c)}{1+\mathcal{P}_\omega\sin^2(\pi\omega/\omega_c)} \tag{4}$$

and

$$B_\omega\simeq\frac{\tau_{\rm tr}}{\tau^*}P_\omega\left[\frac{\pi\omega}{\omega_c}\sin\frac{2\pi\omega}{\omega_c}+\sin^2\frac{\pi\omega}{\omega_c}\right] \tag{5}$$

are dimensionless oscillating functions describing MIROs. The denominator of A_ω accounts for the saturation effect at high enough microwave intensity. Finally,

$$\mathcal{P}_\omega=\frac{\tau_{\rm in}}{\tau_{\rm tr}}P_\omega,\quad P_\omega=\left(\frac{eE_\omega}{\hbar\omega}\right)^2\overline{v_F^2}\frac{\omega_c^2+\omega^2}{(\omega^2-\omega_c^2)^2}. \tag{6}$$

The dimensionless factor P_ω is proportional to the absorbed microwave power. E_ω is the amplitude of electric field of the microwaves, $\overline{v_F^2}=(v_1^2+v_2^2)/2$ is the averaged Fermi velocity (the Fermi velocities in the subbands are defined as $v_j=\hbar k_j/m$), and $\tau_{\rm in}$ is the inelastic relaxation time. This expression for P_ω assumes linear polarization of microwaves and is valid away from the cyclotron resonance.

The general expression is considerably simplified in the case relevant to our DQWs, when $\Delta/2$ is much smaller than the Fermi energy ε_F. In this case one may approximate $n_1\simeq n_2\simeq n_s/2$ and $\nu_{11}\simeq\nu_{22}$, $\nu_{11}^{\rm tr}\simeq\nu_{22}^{\rm tr}$, $\nu_{11}^*\simeq\nu_{22}^*$, which leads also to $\nu_1\simeq\nu_2$, $d_1\simeq d_2$, $\nu_1^{\rm tr}\simeq\nu_2^{\rm tr}\simeq 1/\tau_{\rm tr}$, and $\nu_1^*\simeq\nu_2^*\simeq 1/\tau^*$. Moreover, in balanced DQWs and under condition that interlayer correlation of scattering potentials is not essential, one has[12] $\nu_{12}^{\rm tr}\simeq\nu_{jj}^{\rm tr}$ and $\nu_{12}^*\simeq\nu_{jj}^*$. Applying these approximations to Eq. (1), we rewrite it in the form

$$\frac{\rho_d}{\rho_0}\simeq 1-2\mathcal{T}d\sum_{j=1,2}\cos\frac{2\pi(\varepsilon_F-\varepsilon_j)}{\hbar\omega_c}+d^2[1-A_\omega-B_\omega]\left(1+\cos\frac{2\pi\Delta}{\hbar\omega_c}\right). \tag{7}$$

The second-order quantum contribution (the last term in this expression) is reduced to the corresponding single-subband form[6] if the MIS oscillation factor $1+\cos(2\pi\Delta/\hbar\omega_c)$ is replaced by 2. The amplitude of this contribution is determined by the single squared Dingle factor $d^2=\exp(-2\pi/\omega_c\tau_q)$, where the quantum lifetime is defined as $1/\tau_q\equiv(\nu_1+\nu_2)/2$. The MIROs are given by the term $-A_\omega-B_\omega$ representing a combined action of the inelastic and displacement mechanisms. Since the factor $2\pi\omega/\omega_c$ is large compared to unity in the region of integer MIROs ($\omega>\omega_c$), the functions A_ω and B_ω have nearly the same frequency dependence (if far from the saturation regime) and differ only by magnitude and by different sensitivity to temperature.

The consideration presented above neglects the contribution of the photovoltaic mechanism, which, according to theory, should give a different frequency dependence leading, in particular, to a different phase of MIROs. This contribution decreases with increasing ω. According to our theoretical estimates, the photovoltaic mechanism contribution in our samples can be neglected in comparison to contributions of both inelastic and displacement mechanisms at the frequencies we use, while in samples with higher mobilities its relative contribution is even smaller. Taking also into account that the phase shift in MIROs specific for the photovoltaic mechanism has not been detected experimentally, the neglect of this mechanism is reasonably justified.

For the analysis of experiments, we have to take into account the dependence of the characteristic scattering times: quantum lifetime τ_q and inelastic relaxation time $\tau_{\rm in}$ on the effective electron temperature T_e. According to theory,[6] based on consideration of electron-electron scattering, $\tau_{\rm in}$ scales as

$$\frac{\hbar}{\tau_{\rm in}}\simeq\lambda_{\rm in}\frac{T_e^2}{\varepsilon_F}, \tag{8}$$

where $\lambda_{\rm in}$ is a numerical constant of order unity. To take into account Landau level broadening owing to electron-electron scattering, a similar contribution should be added to inverse quantum lifetime,[16] so $1/\tau_q$ is replaced with $1/\tau_q+1/\tau_q^{ee}\equiv 1/\tau_q(T_e)$, where $\hbar/\tau_q^{ee}\simeq\lambda T_e^2/\varepsilon_F$; the numerical constants $\lambda_{\rm in}$ and λ are not, in general, equal to each other. As a result, the Dingle factor becomes temperature-dependent: $d\to d(T_e)=\exp[-\pi/\omega_c\tau_q(T_e)]$.

For weak microwave power (far from the saturation regime), Eq. (7) can be rewritten in the form

$$\frac{\rho_d}{\rho_0} \simeq 1 + \left.\frac{\rho_d}{\rho_0}\right|_S + d^2(T_e)\left(1+\cos\frac{2\pi\Delta}{\hbar\omega_c}\right) \times\left\{1 - P_\omega\left[[(T_0/T_e)^2+\beta]\frac{2\pi\omega}{\omega_c}\sin\frac{2\pi\omega}{\omega_c} + 2\beta\sin^2\frac{\pi\omega}{\omega_c}\right]\right\}, \quad (9)$$

where the SdH oscillation term from Eq. (7) is denoted as $\rho_d/\rho_0|_S$. In this expression, we have applied the dependence $\tau_{\rm in} \propto T_e^{-2}$ and denoted T_0 as the temperature when $\tau_{\rm in}=\tau_{\rm tr}$. Next, $\beta=\tau_{\rm tr}/2\tau^*$. The contributions proportional to β come from the displacement mechanism. Since the first term in the square brackets is considerably larger than the second one, it dominates the frequency dependence of MIROs. Therefore, the combined action of the inelastic and displacement mechanisms on the magnetoresistance can be approximately described by using the expression for inelastic mechanism contribution with an effective (enhanced owing to the displacement mechanism) relaxation time $\tau_{\rm in}^*$

$$\tau_{\rm in}^* \equiv \tau_{\rm in} + \frac{\tau_{\rm tr}^2}{2\tau^*} = \tau_{\rm tr}[(T_0/T_e)^2+\beta]. \quad (10)$$

The crossover between inelastic and displacement mechanisms should take place at a characteristic temperature $T_C=T_0/\sqrt{\beta}$. Below, we present our experimental results and compare them with the theoretical predictions.

III. RESULTS AND CONCLUSIONS

While similar results have been obtained for various frequencies between 55 and 140 GHz, we focus our analysis on the frequencies 85 GHz (attenuation −7.5 dB) and 110 GHz (attenuation 0 dB). The electric fields for both frequencies, $E_\omega=2$ V/cm (85 GHz, −7.5 dB) and $E_\omega=1.5$ V/cm (110 GHz, 0 dB), and the corresponding (B-dependent) electron temperatures T_e were estimated by comparing the effect of heating-induced suppression of SdH oscillations with a similar effect in the known dc electric fields. At low temperatures, these quantities are in agreement with those obtained by fitting calculated amplitudes of the magnetoresistance oscillations to experimental data.

The theoretical magnetoresistance is calculated as explained above. The temperature dependence of quantum lifetime entering the Dingle factor is determined from temperature dependence of the MIS oscillations in the absence of microwaves (see the details in Ref. 11). This dependence fits well to the theoretically predicted one, where the contribution of electron-electron scattering enters with $\lambda=3.5$ (see previous section). The low-temperature quantum lifetime τ_q caused by impurity scattering is 3.5 ps, which corresponds to the ratio $\tau_{\rm tr}/\tau_q \simeq 15$. The low-temperature magnetoresistance in the presence of microwave irradiation is satisfactory described by the inelastic mechanism contribution with $\tau_{\rm in}$ of Eq. (8), and a comparison of experimental and theoretical

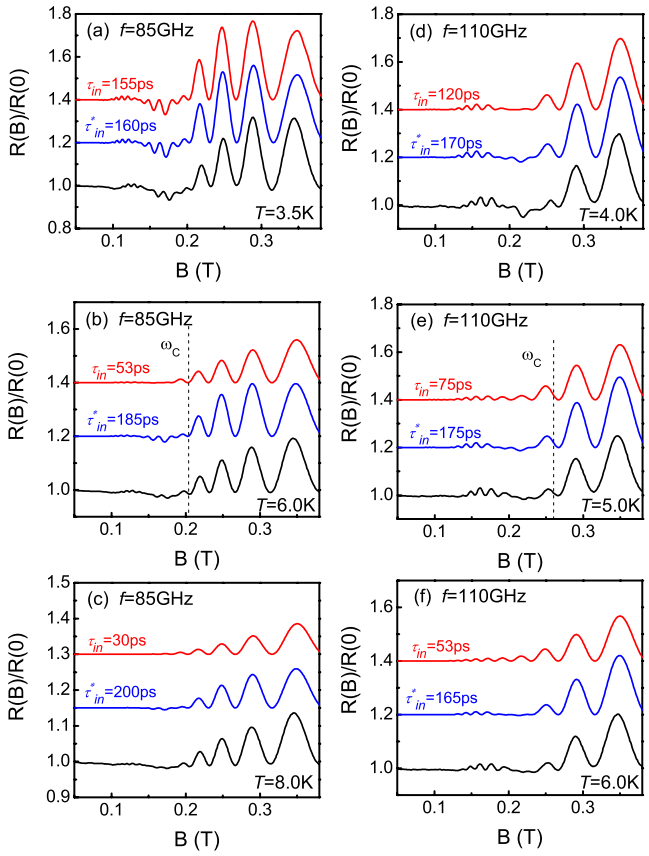

FIG. 2. (Color online) Examples of measured and calculated magnetoresistance for 85 GHz (a–c) and 110 GHz (d–f). Red (top trace) is the theoretical magnetoresistance with the inelastic mechanism contribution. We display corresponding inelastic scattering time for the given electron temperature $T=T_e$. Blue (middle trace) is the theoretical magnetoresistance with an enhanced $\tau_{\rm in}^*$, which fits the experimental data (black, bottom trace). Theoretical curves are shifted up for clarity.

results allows us to determine $\lambda_{\rm in} \simeq 0.94$ in this dependence.

With increasing temperature, the inelastic mechanism alone fails to describe the experimental magnetoresistance, and we have to introduce an enhanced relaxation time $\tau_{\rm in}^*$. This is shown in Fig. 2 where we plot the dc resistivity as a function of B for the inelastic model with corresponding $\tau_{\rm in}$ (red), inelastic model with an enhanced $\tau_{\rm in}^*$ (blue), and experimental trace (black) for several chosen temperatures. For both frequencies, the heating due to microwaves can be neglected for $T \geq 2.8$ K, thus $T \simeq T_e$. It is clearly seen that with increasing temperature, the theoretical model does not fit the magnetoresistance for $0.1\ {\rm T} < B < 0.3$ T. Starting at 85 GHz [Fig. 2(a)–2(c)], we find that neither the flipped MIS peaks around $B=0.17$ T nor the slightly enhanced MIS peaks at $B=0.13$ T occur in the inelastic model if we use calculated inelastic relaxation time $\tau_{\rm in}$. With an enhanced time $\tau_{\rm in}^*$, e.g., in Fig. 2(b), with $\tau_{\rm in}^*=3.5\tau_{\rm in}$, both features appear at the corresponding magnetic field. This deviation is especially clear in Fig. 2(c) at $T=8$ K. Here, we use $\tau_{\rm in}^*=6.7\tau_{\rm in}$ to obtain the closest fit to the experimental result. For 110 GHz, we observe similar results for all temperatures, and we show the features at $T=4$, 5, and 6 K, see Figs. 2(d)–2(f). Due to a

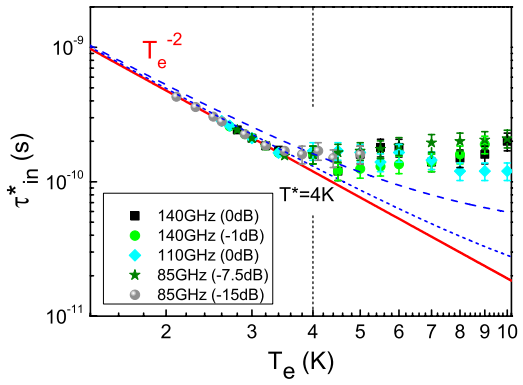

FIG. 3. (Color online) Temperature dependence of the effective relaxation time $\tau^*_{\rm in}$ extracted for different microwave frequencies and intensities (points), and theoretically predicted inelastic relaxation time $\tau_{\rm in} \propto T_e^{-2}$ of Eq. (8) (red thick line). The deviation from the inelastic model starts at a critical temperature $T^* \simeq 4$ K. For higher T_e, we observe an almost temperature-independent behavior until the effect of microwaves on the DQW systems vanishes depending on the strength of the electric field E_ω. The theoretical dependence of $\tau^*_{\rm in}$ under approximations of smooth scattering potential (short dash) and of mixed disorder at maximal possible content of short-range scatterers (dash) are also shown.

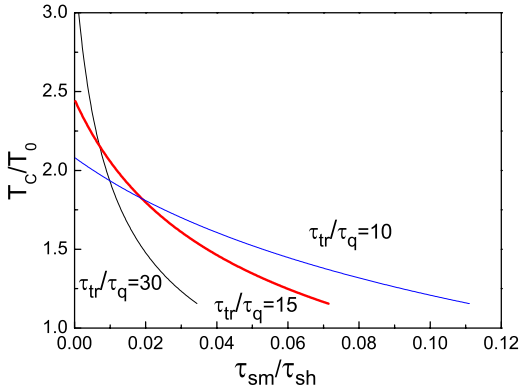

FIG. 4. (Color online) Theoretical dependence of the crossover temperature on the content of short-range scatterers for several given ratios $\tau_{\rm tr}/\tau_q$ (for our sample this ratio is 15). T_0 is the temperature when $\tau_{\rm in}$ equals $\tau_{\rm tr}$.

different frequency, which changes strongly the MIS oscillation picture,[10] we focus now on the enhanced MIS peaks around $B=0.16$ T and the damped features at $B=0.22$ T. Whereas the comparison with theoretical model only shows a slightly smaller amplitude of the enhanced MIS peaks at $B=0.16$ T, the damped or inverted MIS peaks [Fig. 2(d)] observed in experiment at $B=0.22$ T do not occur unless $\tau_{\rm in}$ is enhanced to $\tau^*_{\rm in}$.

In Fig. 3, we show the enhanced relaxation time $\tau^*_{\rm in}$ as a function of electron temperature T_e. We have added the data for a higher frequency of 140 GHz and for a lower microwave intensity (85 GHz at −15 dB, the estimated electric field is $E_\omega=0.8$ V/cm). It is clearly seen that $\tau^*_{\rm in}$ is very close to $\tau_{\rm in} \propto T_e^{-2}$ for $T_e \leq T^*$, which strongly confirms the relevance of the inelastic mechanism of photoresistance in this region of temperatures. The deviation from this mechanism begins at $T^* \simeq 4$ K, which is identified as a "critical" temperature. For $T_e > T^*$, a nearly temperature-independent (constant) $\tau^*_{\rm in}$ is obtained in the whole frequency range. The dispersion of the experimental points in this region of temperatures is attributed to a limited accuracy of our analysis, when temperature dependence of the prefactor is extracted using the expressions containing temperature-dependent exponential factor $d^2(T_e)$. For each extracted $\tau^*_{\rm in}$, we present an error bar in Fig. 3 for $T > 3.5$ K. Note that for low temperature, the errors become smaller due to the T^{-2}-dependence of inelastic relaxation time.

It is tempting to attribute the observed behavior to the theoretically predicted crossover between the inelastic and displacement mechanisms. To check out the reliability of this assumption, let us compare the experimental critical temperature T^* with the theoretical crossover temperature. Based on our experimental data, we find $T_0 \simeq 6.0$ K. To find the parameter β, an additional consideration is required, since the time τ^* is not directly determined from experiment. This time is expressed through the angular harmonics of the scattering rate as[17,18]

$$\frac{1}{\tau^*} = \frac{3}{2\tau_0} - \frac{2}{\tau_1} + \frac{1}{2\tau_2}, \tag{11}$$

while $1/\tau_q = 1/\tau_0$ and $1/\tau_{\rm tr} = 1/\tau_0 - 1/\tau_1$. A large ratio of $\tau_{\rm tr}/\tau_q$, which is typical for modulation-doped structures, suggests that the scattering is caused mostly by the long-range random potential (smooth disorder). If a model of exponential correlation is used [$w(q) \propto \exp(-l_c q)$, where l_c is the correlation length of the random potential], each harmonic is given by the following expression:

$$\frac{1}{\tau_k} = \frac{1}{\tau_{\rm sm}} \frac{1}{1+\chi k^2}, \quad \chi = (k_F l_c)^{-2} \ll 1. \tag{12}$$

Since the parameter χ can be determined from the known ratio $\tau_{\rm tr}/\tau_q$, which is equal to $1+\chi^{-1}$ in this model, the time τ^* and, hence, β can be found. For our samples, we obtain the crossover temperature $T_C \simeq 15.3$ K, which is considerably larger than T^*. Therefore, the displacement mechanism contribution is not strong enough to explain the observed temperature behavior.

Recently, it was shown[18] that the presence of a small amount of short-range scatterers (such as point defects whose radius is much smaller than the inverse Fermi wavenumber $1/k_F$) increases the contribution of the displacement mechanism. For this two-component disorder model, Eq. (12) should be replaced with[17,18]

$$\frac{1}{\tau_k} = \frac{\delta_{k,0}}{\tau_{\rm sh}} + \frac{1}{\tau_{\rm sm}} \frac{1}{1+\chi k^2}. \tag{13}$$

The relative content of the short-range scatterers can be characterized by the ratio $\tau_{\rm sm}/\tau_{\rm sh}$. The crossover temperature T_C, indeed, decreases with increasing $\tau_{\rm sm}/\tau_{\rm sh}$. However, to keep a constant $\tau_{\rm tr}/\tau_q$ determined experimentally, one cannot make $\tau_{\rm sm}/\tau_{\rm sh}$ too large. In Fig. 4, we illustrate the dependence of T_C/T_0 on the content of the short-range scatterers for several ratios of $\tau_{\rm tr}/\tau_q$. Each curve stops at the point when the given ratio cannot be reached if we add more short-

range scatterers; this point corresponds to $\beta=3/4$. Therefore, for two-component disorder we can reduce T_C down to $(2/\sqrt{3})T_0$, which in our case gives the lower limit $T_C \simeq 7$ K. Again, the displacement mechanism contribution is still weak to produce the crossover at $T \simeq 4$ K.

To demonstrate the temperature dependence of the expected τ_{in}^*, we add the theoretical plots based on Eq. (10) with $T_C=15.3$ K and $T_C=7$ K to Fig. 3. It is clear that the smooth disorder model cannot fit the experimental data above $T^*=4$ K. The mixed disorder model produces a better (still not sufficient) agreement with experiment in this region, but leads to a noticeable deviation from the $\tau_{in}^* \propto T^{-2}$ dependence in the region $T<T^*$. This essential observation shows that the behavior of τ_{in}^* can hardly be explained within a model that adds a temperature-independent [as in Eq. (10)] or weakly temperature-dependent term to τ_{in}: such a term cannot lead to a distinct change in the slope of the T-dependence around T^*. Therefore, one may suggest that another, previously unaccounted mechanism of photoconductivity, which turns on at $T \simeq T^*$ more abruptly than the displacement mechanism, should be important.

In conclusion, we have studied the temperature dependence of magnetoresistance oscillations in the systems with two closely spaced 2D subbands (DQWs) under continuous microwave irradiation. With increasing temperature to $T^* \simeq 4$ K, we observe a considerable deviation from the temperature dependence predicted by the inelastic mechanism of microwave photoresistance. A similar behavior (at $T^* \simeq 2$ K) has been recently observed in high-mobility quantum wells with one occupied subband[9] and attributed to a crossover between inelastic and displacement mechanisms.[9,18] We have analyzed our data in terms of this model, by taking into account elastic scattering of electrons by both long-range and short-range impurity potentials. We have found that even in the light of limited accuracy of our analysis, the observed deviation cannot be fully explained by the contribution of the displacement mechanism, and, therefore, requires another explanation. We believe that this finding will stimulate further theoretical and experimental work on the transport properties of 2D electron systems exposed to microwave irradiation.

ACKNOWLEDGMENTS

We thank M. A. Zudov and I. A. Dmitriev for useful discussions. This work was supported by COFECUB-USP (Project No. U$_c$ 109/08), CNPq, FAPESP, and with microwave facilities from ANR MICONANO.

[1] M. A. Zudov, R. R. Du, J. A. Simmons, and J. L. Reno, Phys. Rev. B **64**, 201311(R) (2001).
[2] R. G. Mani, J. H. Smet, K. von Klitzing, V. Narayanamurti, W. B. Johnson, and V. Umansky, Nature (London) **420**, 646 (2002).
[3] M. A. Zudov, R. R. Du, L. N. Pfeiffer, and K. W. West, Phys. Rev. Lett. **90**, 046807 (2003).
[4] V. I. Ryzhii, Fiz. Tverd. Tela (Leningrad) **11**, 2577 (1969) [Sov. Phys. Solid State **11**, 2078 (1970)]; V. I. Ryzhii, R. A. Suris, and B. S. Shchamkhalova, Fiz. Tekh. Poluprovodn. **20**, 2078 (1986) [Sov. Phys. Semicond. **20**, 1299 (1986)].
[5] A. C. Durst, S. Sachdev, N. Read, and S. M. Girvin,Phys. Rev. Lett. **91**, 086803 (2003).
[6] I. A. Dmitriev, M. G. Vavilov, I. L. Aleiner, A. D. Mirlin, and D. G. Polyakov, Phys. Rev. B **71**, 115316 (2005).
[7] I. A. Dmitriev, A. D. Mirlin, and D. G. Polyakov, Phys. Rev. B **75**, 245320 (2007).
[8] S. A. Studenikin, M. Potemski, A. Sachrajda, M. Hilke, L. N. Pfeiffer, and K. W. West, Phys. Rev. B **71**, 245313 (2005).
[9] A. T. Hatke, M. A. Zudov, L. N. Pfeiffer, and K. W. West, Phys. Rev. Lett. **102**, 066804 (2009).
[10] S. Wiedmann, G. M. Gusev, O. E. Raichev, T. E. Lamas, A. K. Bakarov, and J. C. Portal, Phys. Rev. B **78**, 121301(R) (2008).
[11] N. C. Mamani, G. M. Gusev, T. E. Lamas, A. K. Bakarov, and O. E. Raichev, Phys. Rev. B **77**, 205327 (2008).
[12] O. E. Raichev, Phys. Rev. B **78**, 125304 (2008).
[13] N. C. Mamani, G. M. Gusev, E. C. F. da Silva, O. E. Raichev, A. A. Quivy, and A. K. Bakarov, Phys. Rev. B **80**, 085304 (2009).
[14] S. A. Mikhailov, Phys. Rev. B **70**, 165311 (2004).
[15] S. Wiedmann, N. C. Mamani, G. M. Gusev, O. E. Raichev, A. K. Bakarov, and J. C. Portal, Phys. Rev. B **80**, 245306 (2009).
[16] G. F. Giuliani and J. J. Quinn, Phys. Rev. B **26**, 4421 (1982).
[17] M. Khodas and M. G. Vavilov, Phys. Rev. B **78**, 245319 (2008).
[18] I. A. Dmitriev, M. Khodas, A. D. Mirlin, D. G. Polyakov, and M. G. Vavilov, Phys. Rev. B **80**, 165327 (2009).